Near surface characterization using a 9-component refraction survey: Cochrane, Alberta

Darryl G. Parry and Don C. Lawton

ABSTRACT

A 9-component refraction survey was undertaken in the town of Cochrane. The investigated stratigraphy includes fluvial deposits of the Bow River and bedrock. The source employed for this experiment was a wooden beam stuck by a large hammer. This source suffers in the S_V mode from abundant generation of horizontal P-waves. The first break data were obtained by stacking and subtracting same polarity and opposite polarity records, giving a suite of traveltime data. Traveltime data have been interpreted to yield a velocity/depth structure for the survey location. P-wave data imaged the water table at about 14 m depth (V_P = 910 m/s above and 2660 m/s below). SH-wave data do not show the water table, but show the bedrock at about 26 m (V_{SH} = 520 m/s above the bedrock and 1000 m/s within it). A more complete survey would include more shot offsets in order to apply more sophisticated interpretation schemes.

INTRODUCTION

Geotechnical investigations and reflection seismology obtain benefit from the careful interpretation of refraction data (including direct and refracted arrivals of seismic waves). In the first case, the refraction recording is the end product of a survey, in the second it is information ancillary to seismic reflections. Geotechnical refraction surveys have as their goal an accurate interpretation of velocity and depth structure in the near-surface. Time compensation for variable velocity and/or thickness of the weathering layer - static corrections - are the required product of refraction interpretation pursued in conjunction with reflection processing. This difference in focus has led to the development of different interpretation schemes depending on the desired result of the refraction study. A well defined velocity/depth model will readily produce static corrections, but well-defined statics need not produce a velocity/depth model.

A method to obtain statics from refraction data (generalized linear inversion - GLI) is discussed by Hampson and Russell (1984). This technique is a computer-intensive procedure where an estimated earth model is input, the arrival times for the model are calculated and compared to measured values. The model is then perturbed according to the calculated error. Successive iterations are performed until the error is reduced to some acceptable level. The quality of the result depends on an abundance of input data (which CMP profiling provides) and on the accuracy of the initial model.

Velocity/depth structure can be obtained in a variety of ways depending on the nature of the gathered data and the complexity of the near-surface. If the survey is uni-directional (one shot location), the slope-intercept method is all that may be applied. This technique assumes a horizontally layered earth. Velocity is calculated as the reciprocal of the slope of the time-distance (t-x) or traveltime curves. Each unique

slope is interpreted as a separate horizon. Equations for calculating depth are readily available (eg. Palmer, 1986).

The assumptions inherent in the slope-intercept method are based on a grossly oversimplified earth model. Resolution of more detail can be obtained by methods employing shots from both ends of a receiver spread; ie. reciprocal methods. The first benefit of such an application is the potential to identify dipping beds. If the velocity calculated for a layer differs according to shot location, dipping strata are suggested. The shot yielding the higher apparent velocity is on the down dip end of the receiver spread. Equations for calculating dip and depth are presented by Telford et al (1976) and Palmer (1986). Layer velocity is the harmonic mean of the two apparent velocities. This technique still assumes planar strata, but accounts for dip.

Further complexities may be resolved by the use of the plus-minus method (Hagedoorn, 1959; Hawkins, 1961) or the generalized reciprocal method (Palmer, 1981). These techniques provide depth estimates along the spread in addition to depths at the shot points. The resulting depths are not necessarily zero offset. The depth sections can be migrated (in a sense) by constructing arcs whose radii are equal to the calculated depths. The envelope of tangents to these arcs is then the migrated depth section (Palmer, 1980).

Acquisition parameters should be tailored to suit the anticipated structure. Geophone spacing and the near offset need to be chosen so that direct arrivals can be observed over several traces. Reciprocal records improve interpretability and still more can be gained with more source points. By employing near and far offset shots on both ends of the spread, coverage of deeper refractors can be extended (Lankston, 1990). A shot in the middle of the spread may assist in defining the upper layer velocity. These considerations are especially important if the generalized reciprocal method (GRM) or plus-minus method are the techniques used in interpretation.

FIELD PROGRAM

A 9-component refraction survey was performed in August of 1990 as a practical exercise for the University of Calgary Geophysics Field School. The test site (Figure 1) was within the town limits of Cochrane, in the Bow River valley, north of the present stream channel. This location is adjacent to an industrial area in which creosote was used to preserve wood. The study may allow us to determine likely pathways of DNAPL and LNAPL flow, particularly whether the river is likely to become contaminated by any leaking creosote. The near-surface stratigraphy here consists of fluvial gravel terraces overlying sandstone (Jackson et al., 1982).

Three-component OYO receivers were used for the test. The spread geometry was end-on, with an 8 m near offset and 16 receivers laid out at a trace spacing of 8 m giving a source to source spread length of 136 m (Figure 2). The radial geophones were oriented northward and the transverse geophones eastward. The line was oriented north-south (roughly perpendicular to the trend of the river valley).

The source employed was a hammer striking a wooden beam (Figure 3). The dimensions of the beam are 0.3x0.3x3 m. Strips of angle iron attached to its base provide ground coupling for shear-wave generation. Five shot orientations (Figure 4) were used at each of two source points providing three source mode records for each source location. For the shear modes, the hammer was mounted on a pivot on the cage

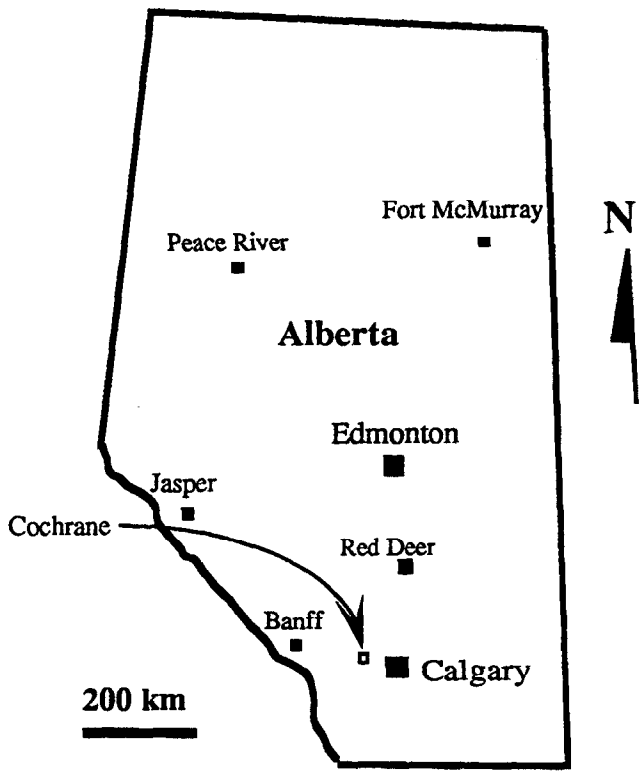

FIG. 1. Alberta map showing location of survey.

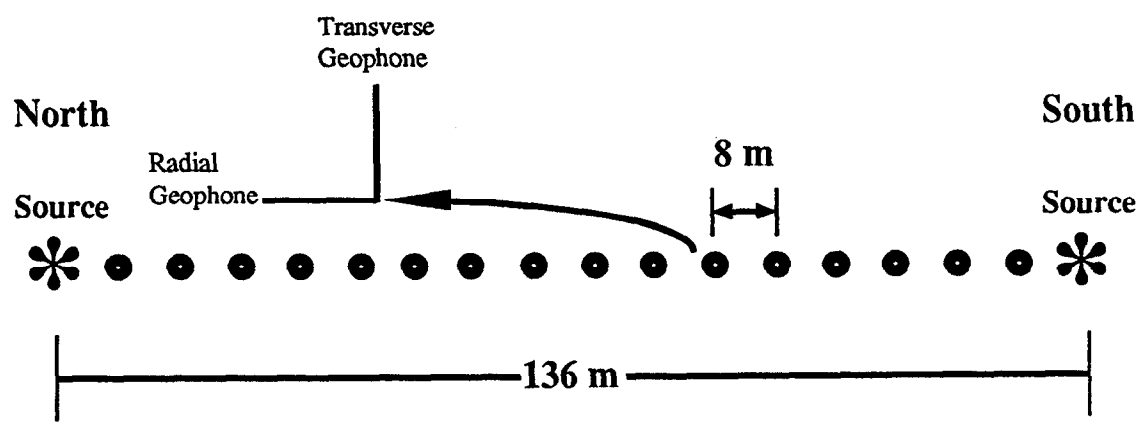

FIG. 2 Refraction survey acquisition geometry.

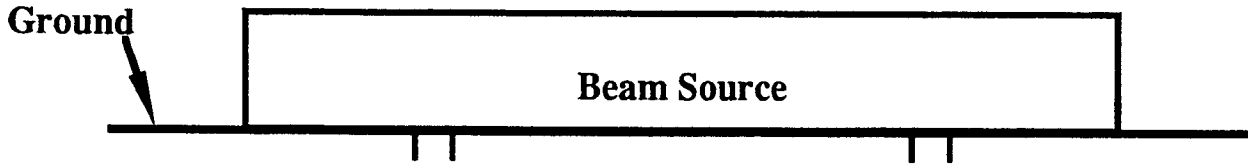

FIG. 3. Schematic diagram of source beam. Side view.

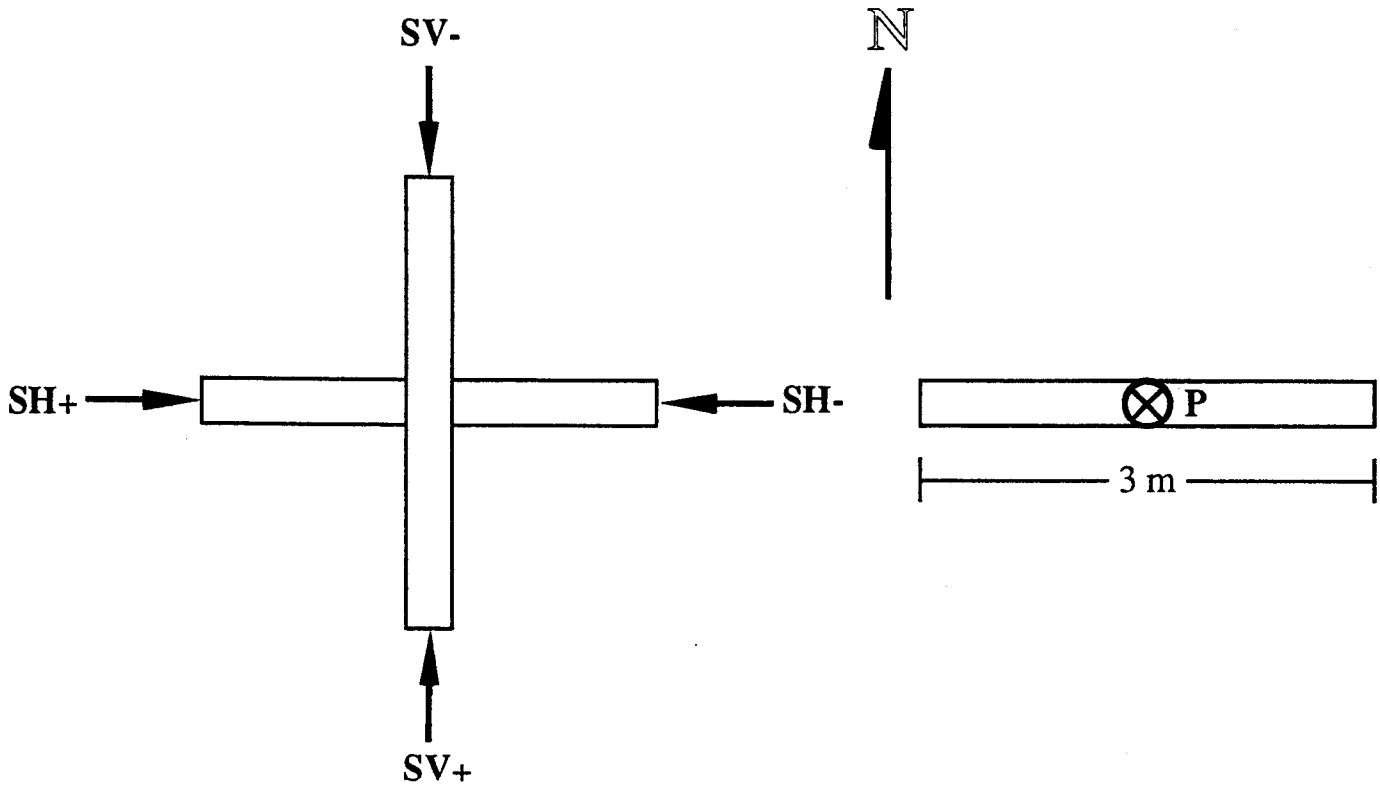

FIG. 4. Map view of source orientations.

of a 1-ton cable truck which was driven up onto the beam. The hammer was then dropped from a fixed height as many as 15 times for each orientation. With the beam oriented north-south (inline) it acted as an SV source. With the beam oriented east-west, it acted as an SH source. Opposing polarity modes were recorded to facilitate data reduction. Recording on the DFS III system was triggered by an "uphole" geophone attached to the beam.

DATA PROCESSING

After demultiplexing, the field data were subjected to a number of processes in an attempt to improve their interpretability. All records for each source mode were first vertically stacked to improve signal to noise ratio. For stacking, the first record in each mode is accepted as the pilot. All ensuing records for that mode are cross-correlated with the pilot to obtain a time-shift resulting from inconsistent triggering from record to record. While most records required time-shifts of 4 ms or less, the time-shift for the SH+ mode from the south source point was as high as 12 ms. The calculated shift was applied and the records were stacked. Not all source modes stacked the same number of records. Amplitudes were normalized according to the number of records stacked before output.

The resulting data set contains four shear mode records and one P for each shot. The opposite polarity SH modes (i.e. SH+ and SH-) can then be summed or subtracted to enhance P or S waves. If they are summed, the shear wave information should add 180° out of phase leaving only a compressional record. If they are subtracted, the P-wave should add out of phase leaving an S-wave record (Lawton, 1990). Amplitudes were normalized for subtraction and summation similarly to stacking.

The final-interpretation data volume then consisted of 6 records (the P record from the vertical channel - P/V; the SV record from the radial channel - SV/R; and the SH record from the transverse channel - SH/T). A 300 ms AGC and 10/20-70/105 Hz bandpass filter were applied prior to interpretation. Ground roll removal via *f/k* filtering was unsuccessful in improving the quality of the first break data as were attempts at deconvolution. Even muting the ground roll showed little improvement in first break interpretability.

RESULTS

Figures 5 and 6, respectively, are plots of the raw records before and after 300 ms AGC. There is some energy on all records suggesting that either the source or the geophones were not exactly oriented, or that the near-surface is anisotropic in the area of the survey. A substantial amount of this energy is from ground roll. The transverse geophone contains much less energy for the P and SV modes than do any of the other records, largely because of differences in the nature of the ground roll. In each case more energy appears on the component matched with a source (i.e. P/V, SV/R, SH/T).

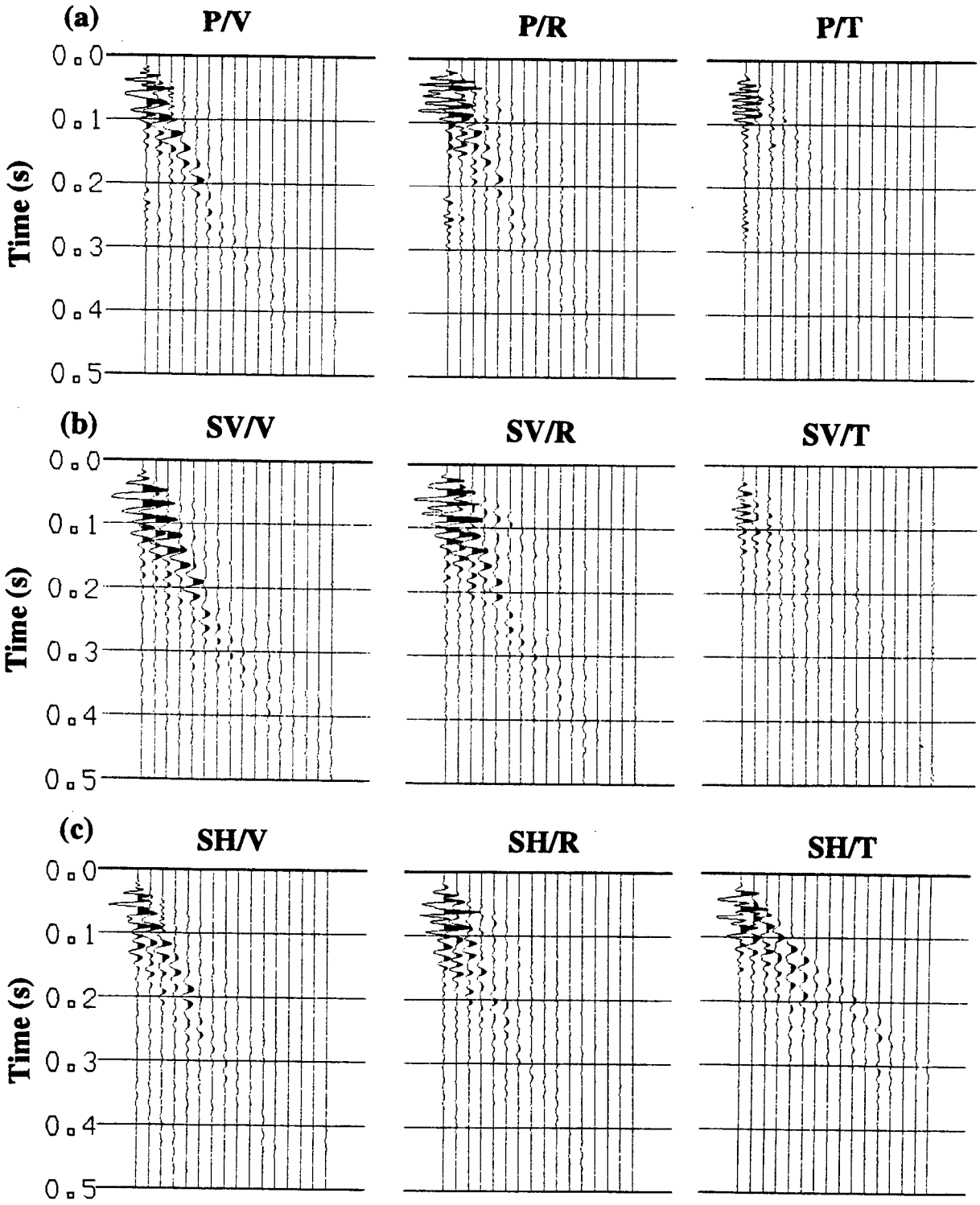

Fig. 5 Raw field records.

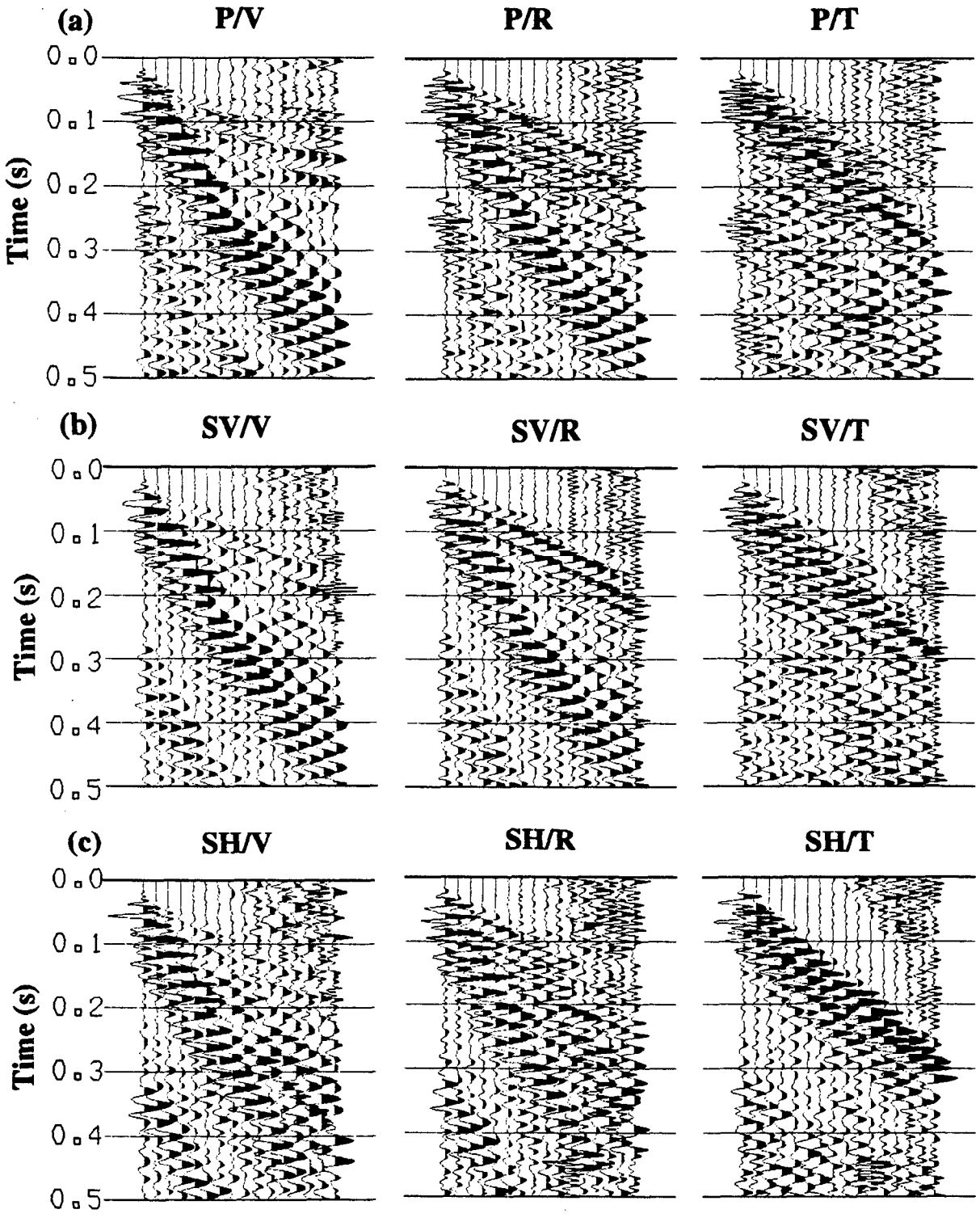

Fig. 6 Raw field records - 300 ms AGC.

Results of processing the SH-mode records are shown in Figure 7; 7(a) are the records obtained by stacking only the SH mode, 7(b) are the subtracted records (SH- - SH+), and 7(c) are the summed records. The shear records for subtraction show slight improvement over the raw stack, and while the headwave is reduced on the vertical record, it is not eliminated. The Rayleigh wave is only slightly diminished. The summation records also show only slight improvement. The P headwave is more interpretable on this record (SH/V) than on the previous two V records and the Rayleigh wave is enhanced. At the same time the Love wave is reduced on the T record and substantially reduced on the R. The summation and differencing techniques do improve data quality, but not to the degree shown elsewhere (Lawton, 1990). This may be largely due to ground roll.

Figure 8 exhibits the full 9-component suite obtained from the south source location in this experiment. The most readily interpretable records are P/V, SV/R, and SH/T. These are the records whose source polarization most closely matches the receiver orientation.

VELOCITY STRUCTURE

The interpretable data volume is presented in Figure 9; 9(a) are from the north located source and 9(b) are from the south. The traveltime data obtained from these records are given in Table 1. The SV/R record trace 6 is dead as that geophone recorded exclusively noise for all of the northern records.

Trace	Offset	P north	P south	SV north	SV south	SH north	SH south
	(m)	(ms)	(ms)	(ms)	(ms)	(ms)	(ms)
1	8	78	5	137	10	214	14
2	16	75	15	131	17	205	30
3	24	24	71	117	30	197	47
4	32	66	38	112	40	189	62
5	40	64	47	104	50	182	80
6	48	60	53	-	59	168	95
7	56	56	56	87	67	153	105
8	64	53	54	78	78	137	117
9	72	50	59	69	87	120	137
10	80	48	60	62	99	108	151
11	88	43	68	51	107	90	169
12	96	44	68	44	116	76	184
13	104	36	72	34	120	59	192
14	112	28	70	25	126	44	196
15	120	20	72	16	133	30	206
16	128	6	77	6	142	11	217

Table 1. Traveltime Data.

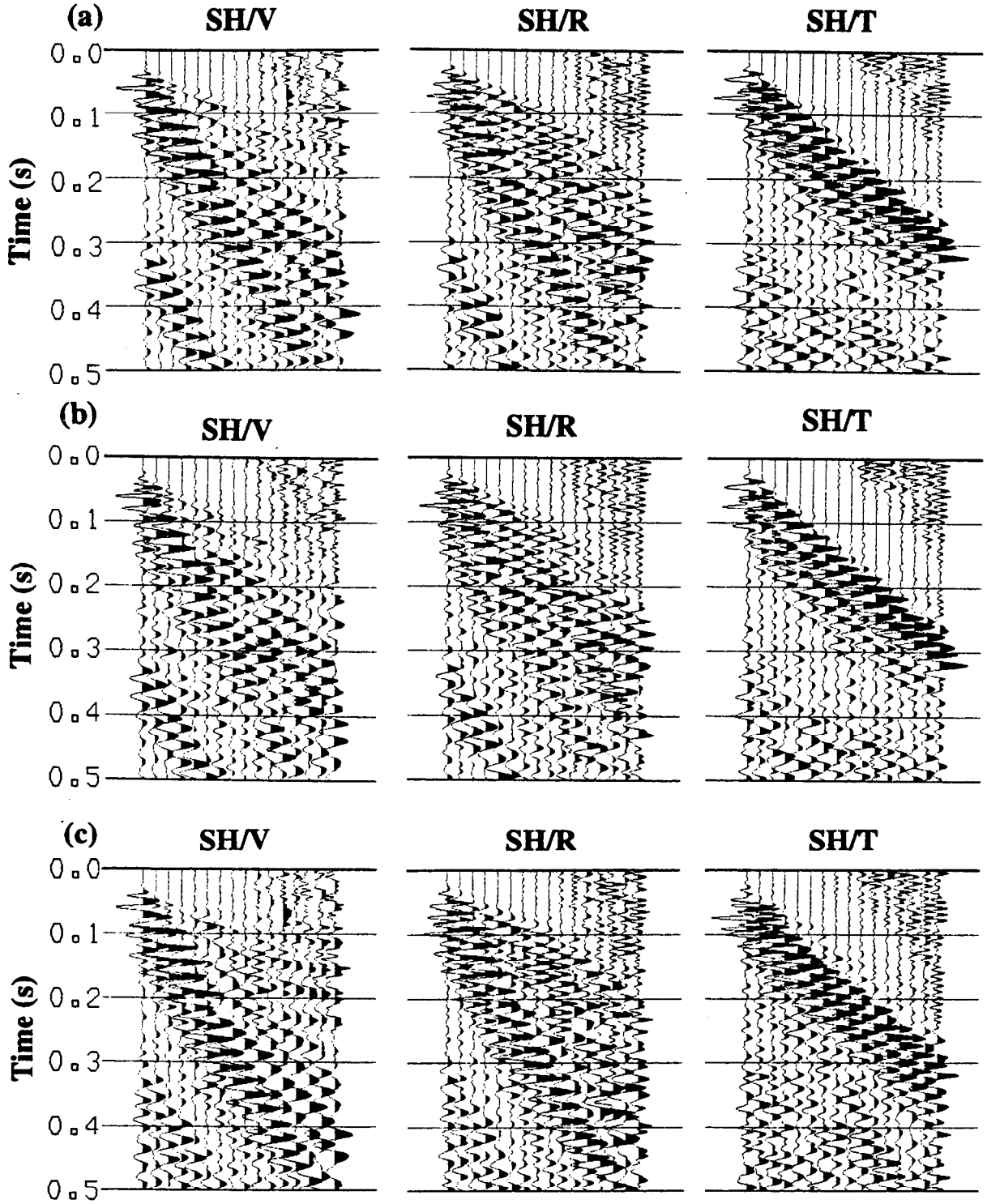

Fig. 7 SH mode records. (a) pure stack, (b) subtraction of opposing polarity sources, (c) summation of opposing polarity sources.

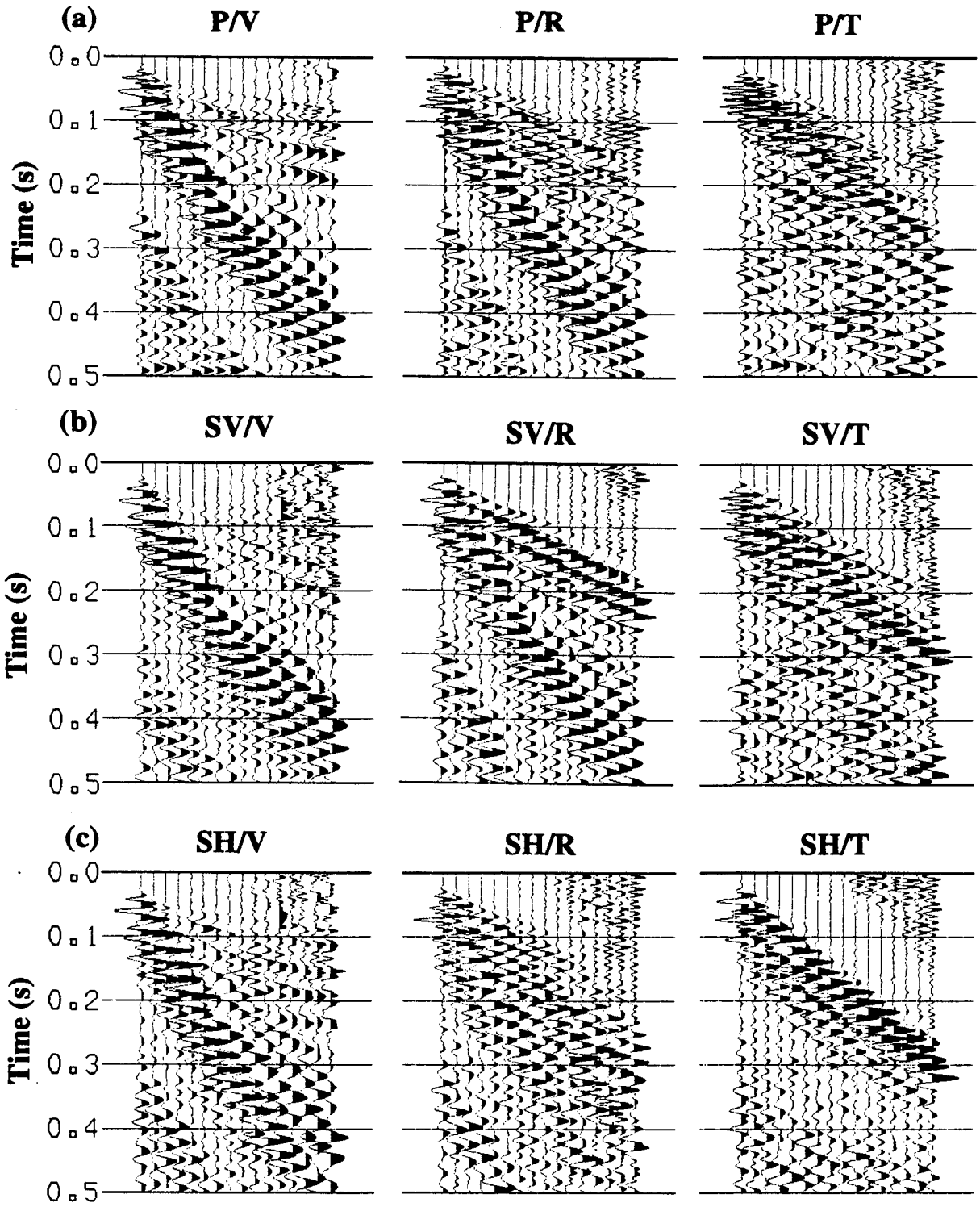

Fig. 8 Full 9-component suite - south source location.

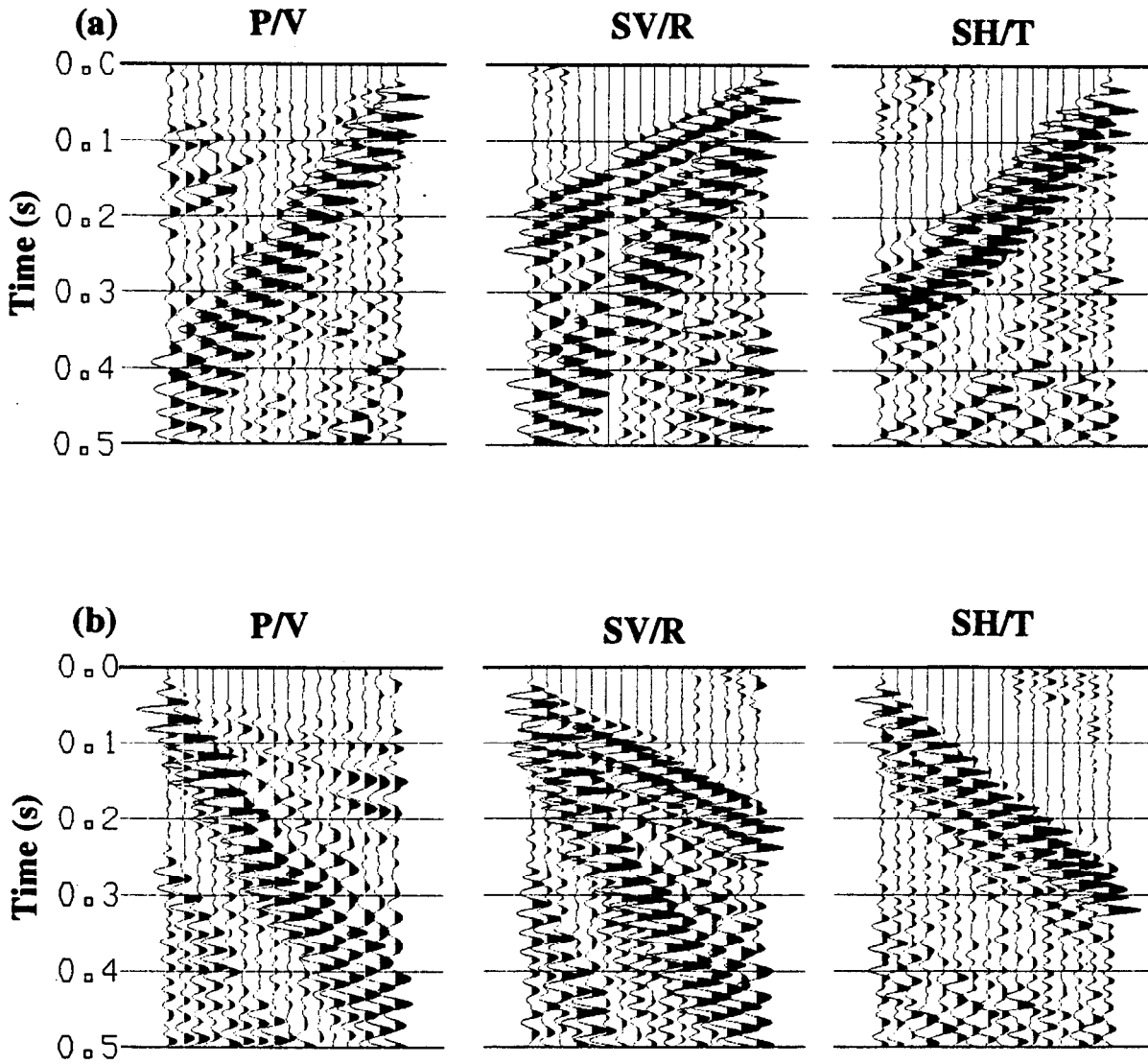

Fig. 9 Processed data volume. (a) north source. (b) south source.

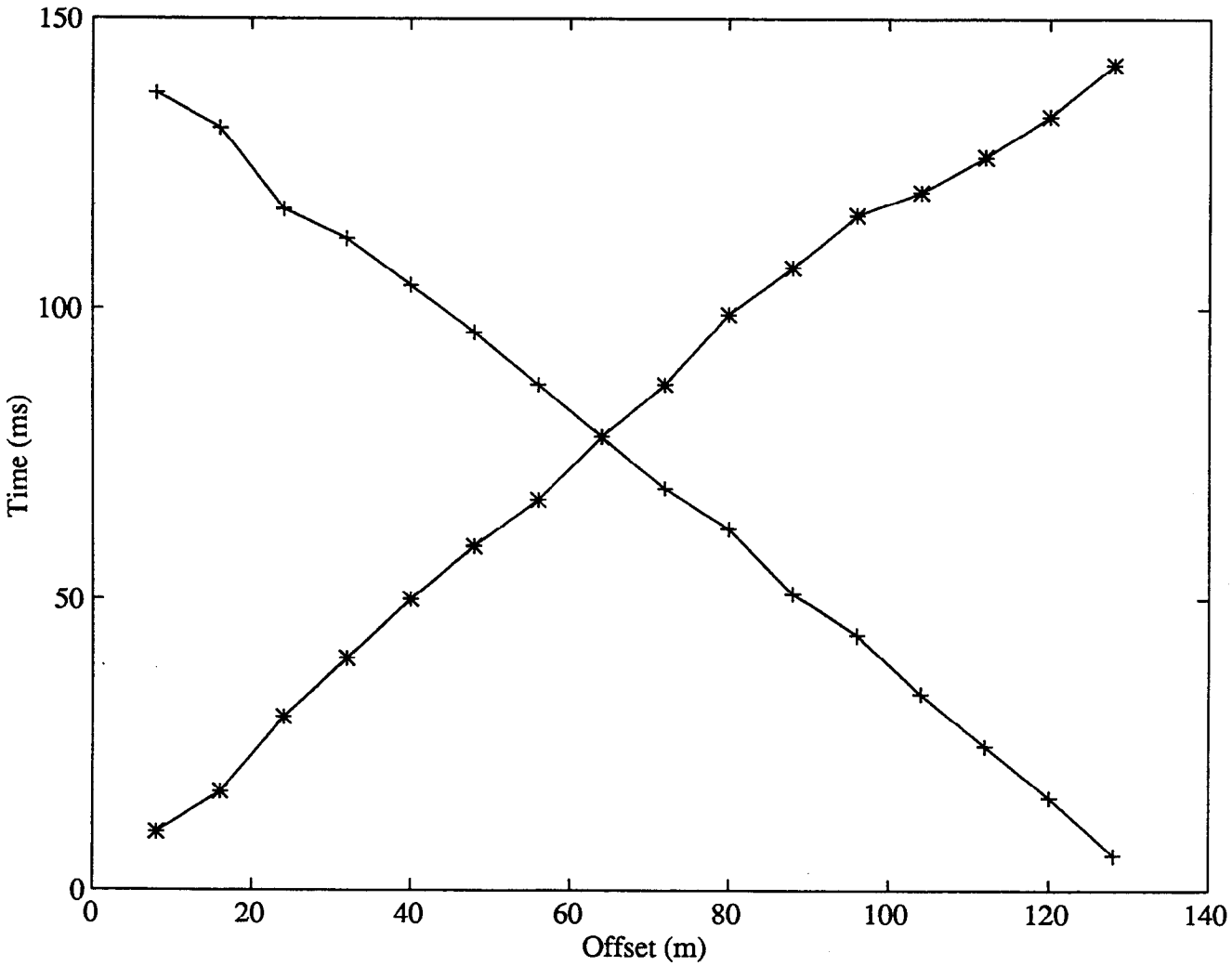

Fig. 10 First arrival traveltime curves for SV record. South source at 0 m. North source at 136 m.

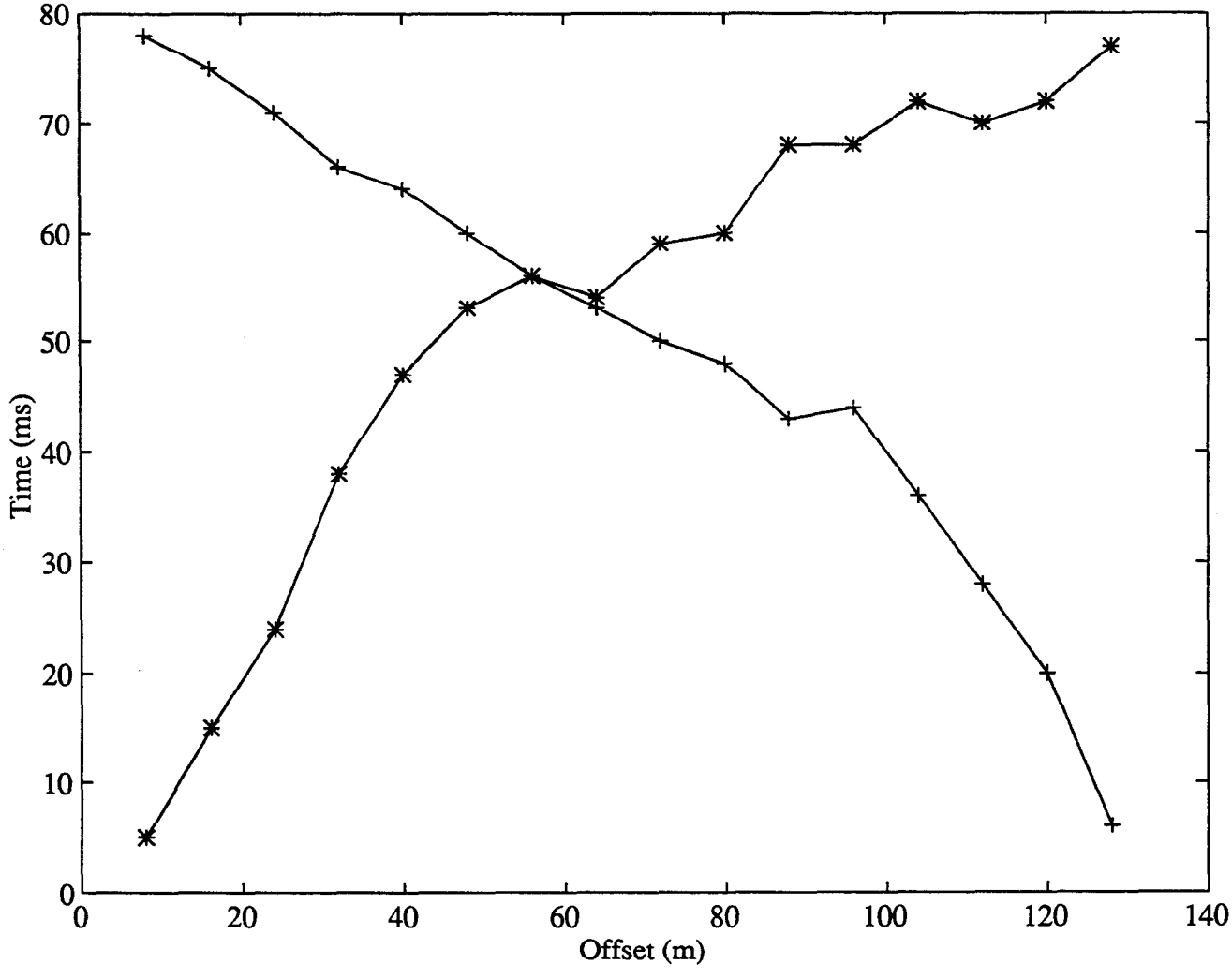

Fig. 11 First arrival traveltime curves for P record. South source at 0 m. North source at 136 m.

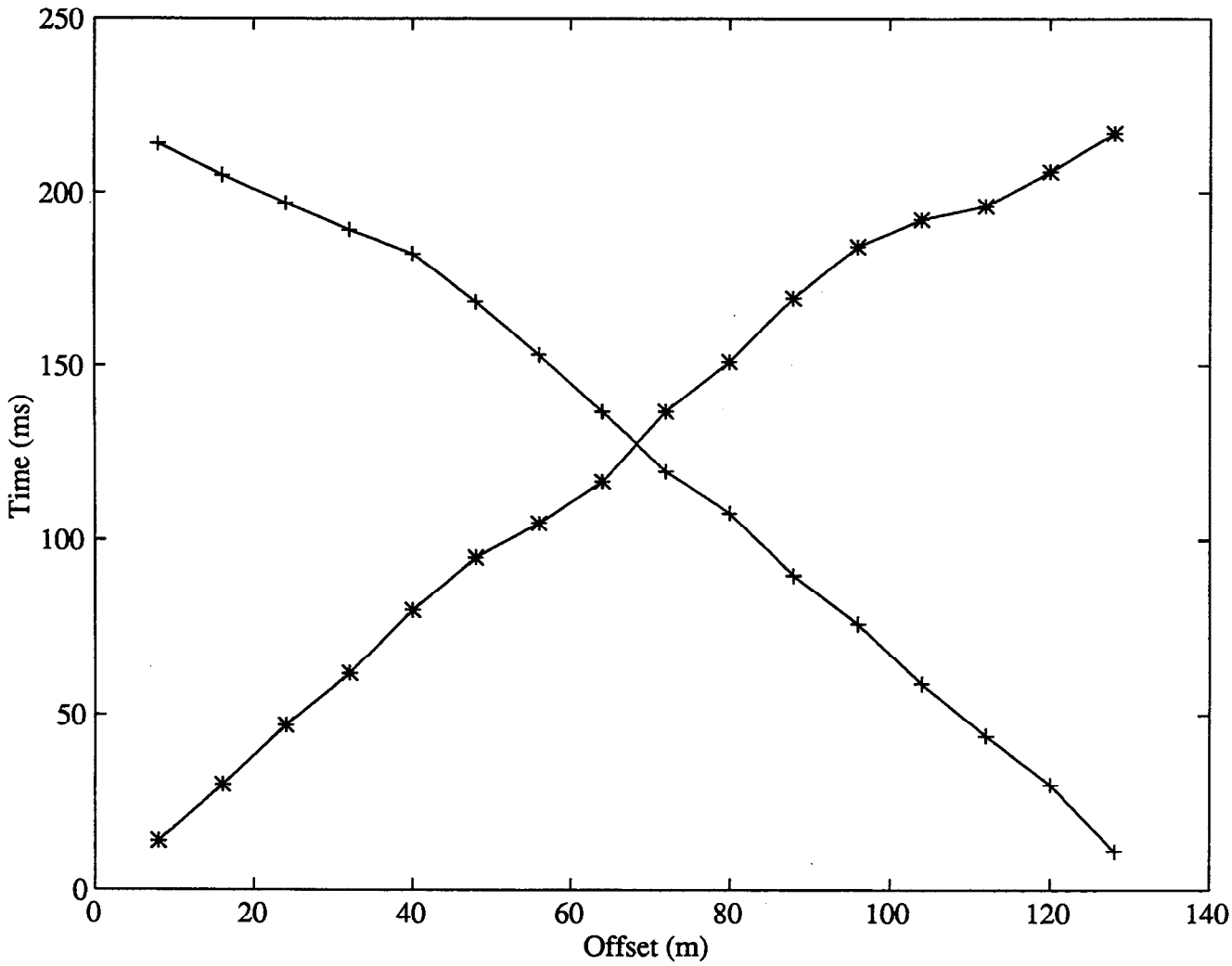

Fig. 12 First arrival traveltime curves for SH record. South source at 0 m. North source at 136 m.

The SV first arrivals seem quite linear. There is a change in slope for P at trace 6 (south source) and trace 11 (north source) suggesting a two layer earth model. SH records also suggest a two layer earth with velocity changes at trace 12 (south source) and trace 6 (north source). Traveltime graphs (Figures 10 - 12) reinforce these interpretations.

There is no plus-minus window (a laterally continuous zone in which a refractor is sampled by data from shots on both ends of the spread) on the SH or SV traveltime curves so only elementary interpretation schemes can be used for these data. The method used was the slope/intercept method considering dipping strata. The SH graph suggests a dip to the north with an upper layer velocity of 520 ± 20 m/s and a lower layer velocity of 1000 ± 30 m/s. Depth to the top of the second layer is 25 m at the north source and 28 m at the south. The error estimates are based on scatter on the traveltime curves. The SV graph yields a single layer velocity of 870 ± 30 m/s.

A plus-minus window exists for the P traveltime data, but the scatter within the window is extreme and a number of the data points are suspect. A simple dipping refractor model was interpreted from these data. The results of this model give an upper layer velocity of 910 ± 20 m/s and a lower layer velocity of 2 660 ± 100 m/s. The depth to the top of the refractor is 11 m at the north source and 17 m at the south.

It is difficult to reconcile the extreme difference between the SH and SV upper layer velocity as well as the similarity between the upper P velocity and the upper SV velocity if we accept that the first break recorded on the radial receivers is produced by an shear wave. This, in fact, does not appear to be the case. It appears that P waves are being produced by the SV source and propagating horizontally. That is, a P wave is being radiated sub-horizontally with the source oriented in-line with the receivers. The P and SV velocity values are within measurement error of each other. If SV refracted arrivals do appear on the record and there is no strong anisotropy in the lower (shear) layer, their velocity will be very close to that of the direct arriving P which may make them indistinguishable. Looking back at Figure 8 there is a marked similarity between the unmatched records P/R and SV/V. It appears that the apparent SV first breaks are in fact P direct arrivals (and possibly refracted SV toward the longer offsets). This is consistent with other reports (Lawton, 1990).

The velocity/depth structure is then a dry upper layer (layer 1) with V_P = 910 m/s and V_{SH} = 520 m/s, the wet layer 2 with V_P = 2660 m/s and V_{SH} = 520 m/s, and the bedrock layer with V_{SH} = 1000 m/s - undetected on P. A longer offset shot would be required to image a P refractor at approximately the same depth as the bottom most SH refractor. The structure is illustrated in Figure 13. Velocity and related parameters are listed in Table 2.

	V_P	V_{SH}	V_P/V_{SH}	σ
	m/s	m/s		
Layer 1	910	520	1.8	0.26
Layer 2	2660	520	5.1	0.48
Layer 3	-	1000	-	-

Table 2. Velocity structure and associated parameters (σ = Poisson's ratio).

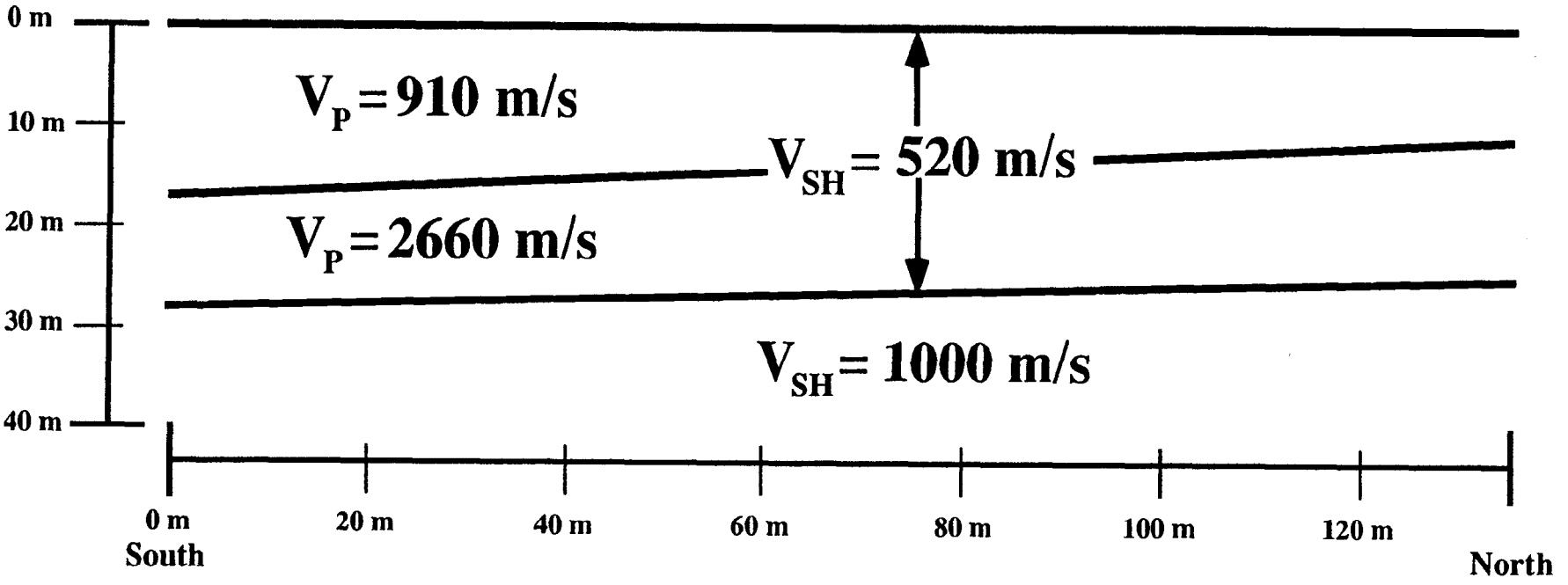

FIG. 13. Velocity/Depth model for P and SH waves.

DISCUSSION

The substantial difference in near-surface P and S velocity structure will result in profoundly different static values for different kinds of reflection surveys. PP static shifts vary from 35 to 46 ms, the SHSH static from 96 to 108 ms, and the converted static PSH from 65 to 77 ms. Multicomponent reflection surveying can be made more accurate by accounting for this variation.

SV velocity structure may be resolvable but, if the beam source is used, longer offsets will be necessary.

The *VP/VS* ratio is expected to be much lower in the unsaturated than in the saturated zone. Shear wave propagation is only supported by the matrix and so shear velocity is largely unaffected by pore fluids. Compressional waves travel through both the solid and the liquid fraction and so are significantly affected by saturation (Stumpel et al., 1984). This explains the survey results which show the water table as a P refractor while it is transparent to the shear.

CONCLUSIONS

The S-wave velocity of dry sediments is 520 m/s as it is for the same sediments below the water table. P-wave velocity changes from 910 m/s above the water table to 2660 m/s below. A third layer is imaged by SV data but not by P. The water table averages 14 m in depth and the bedrock occurs at about 26 m.

SV data is obscured by a horizontally propagating P-wave direct arrival generated while operating the source in SV mode. Farther offsets might allow imaging of deeper refractors with SV, provided that they are of higher velocity than the near-surface P. No comment can be made on anisotropy.

Longer offsets are advisable if the nature of the information required is geotechnical. Implementation of a full reciprocal interpretation scheme would then be feasible. Smaller offsets (eg. mid-spread sources) would also be useful for better definition of the uppermost layers.

REFERENCES

Hagedoorn, J.G., 1959, The plus-minus method for interpreting seismic refraction sections: Geophysical Prospecting, **7**, 158-182.

Hampson, D. and Russell, B., 1984, First-break interpretation using generalized linear inversion: Journal of the Canadian Society of Exploration Geophysics, **20**(1), 40-54.

Hawkins, L.V., 1961, The reciprocal method of routine shallow seismic refraction investigations: Geophysics, **26**, 806-819.

Jackson, L.E.Jr., MacDonald, G.M., and Wilson, M.C., 1982, Paraglacial origin for terraced river sediments in Bow Valley, Alberta: Canadian Journal of Earth Sciences, **19**(12), 2219-2231.

Lankston, R.W., 1990, High-resolution refraction seismic data acquisition and interpretation; in, Ward, S.H., Ed., Geotechnical and Environmental Geophysics: Volume I - Review and Tutorial: Society of Exploration Geophysicists

Lawton, D.C., 1990, A 9-component refraction seismic experiment: Canadian Journal of Exploration Geophysics, **26**(1&2) 7-16.

Palmer, D., 1980, The generalized reciprocal method of seismic refraction interpretation: Society of Exploration Geophysicists

--------, 1981, An introduction to the generalized reciprocal method of seismic refraction interpretation: Geophysics, **46**(11), 1508-1518.

--------, 1986, Refraction seismics; the lateral resolution of structure and seismic velocity: Geophysical Press.

Stumpel, H., Kahler, S., Meissner, R., and Milkereit, B., 1984, The use of seismic shear waves and compressional waves for lithological problems in shallow sediments: Geophysical Prospecting, **32**(4), 662-675.

Telford, W.M., Geldart, L.P., Sheriff, R.E., and Keys, D.A., 1976, Applied geophysics: Cambridge University Press.